Materials Science and Engineering B 176 (2011) 1128–1131

Contents lists available at ScienceDirect

Materials Science and Engineering B

journal homepage: www.elsevier.com/locate/mseb

Short communication

Inkjet-printing of indium tin oxide (ITO) films for transparent conducting electrodes

Myun-sung Hwang[a,b], Bong-yong Jeong[a], Jooho Moon[b], Sang-Ki Chun[c], Jihoon Kim[a,*]

[a] Future Convergence Ceramic Division, Korea Institute of Ceramic Engineering and Technology, Seoul 153-801, Republic of Korea
[b] Department of Advanced Materials Engineering, Yonsei University, Seoul 120-749, Republic of Korea
[c] Research Park, LG Chem., Daejeon 305-380, Republic of Korea

ARTICLE INFO

Article history:
Received 21 December 2010
Received in revised form 28 March 2011
Accepted 22 May 2011

Keywords:
Inkjet
Printing
ITO
Ag-grid

ABSTRACT

Indium-tin-oxide (ITO) films have been prepared by inkjet-printing using ITO nanoparticle inks. The electrical and optical properties of the ITO films were investigated in order to understand the effects of annealing temperatures under microwave. The decrease in the sheet resistance and resistivity of the inkjet-printed ITO films was observed as the annealing temperature increases. The film annealed at 400 °C showed the sheet resistance of 517 Ω/sq with the film thickness of ~580 nm. The optical transmittance of the films remained constant regardless of their annealing temperatures. In order to further reduce the sheet resistance of the films, Ag-grid was printed in between two layers of inkjet-printed ITO. With 3 mm Ag-grid line-to-line pitch, the Ag-grid inserted ITO film has the sheet resistance of 3.4 Ω/sq and the transmittance of 84% after annealing at 200 °C under microwave.

1. Introduction

Printing technology recently attracts substantial attention from various microelectronic applications, especially in the field of optoelectronics such as flexible displays, touch panels, solar cells [1–5]. Such a considerable interest is attributed to the fact that the printing technology results in simpler and more eco-friendly fabrication processes with lower process cost compared to the conventional vacuum-based fabrication processes [6–10].

Transparent conducting oxide (TCO) is one of the most indispensable materials to fabricate the optoelectronic devices. Most of TCO films, currently, have been prepared by vacuum-assisted process such as DC and RF sputtering. However, their high loss of the target materials during sputtering prevents the sputtering process from further reducing the fabrication cost as well as the expense for the treatment of anti-environmental wastes. Many efforts have been devoted to synthesizing TCO films by solution-based processes such as spray pyrolysis, dip-coating, spin coating, casting [11–14]. However, these processes are still limited in terms of producing selective deposition of TCO films on the desired area. From these aspects, the direct pattering by printing technology is much beneficial to the fabrication of optoelectronic devices. Among various printing technologies, inkjet printing is known as a non-contact additive process which deposits the desired amount of various functional materials directly from computer design images onto the selected area of the substrates without any contamination [15]. So, in this paper, we have selected the inkjet printing as a printing technique for the fabrication of ITO films.

Among various TCO materials, indium-tin-oxide (ITO) is considered most promising for the various optoelectronic applications such as liquid crystal displays, plasma display panels, organic light emitting diodes, touch panels, solar cells. Since it shows low electrical resistivity in conjunction with high transmission in the visible spectra. The low resistivity of ITO is attributed to the degeneracy resulting from its high carrier concentration by oxygen vacancy as well as tin dopants [16]. The high transparency of ITO comes from its wide band gap ranging from 3.5 eV to 4.3 eV [17]. In this work, we present feasibility on the inkjet-printing of high-performance ITO films. The optical and electrical properties of the inkjet-printed ITO films were investigated depending upon the rapid thermal annealing condition. We also introduced Ag-grid lines to the inkjet-printed ITO films. Ag-grid lines were patterned by inkjet in between two inkjet-printed ITO films in order to understand its effects on the electrical and optical properties of the films.

2. Experimental procedure

Commercial ITO nano-particles with D_{50} = 25 nm (Advanced Nano Products) were utilized in ITO ink formulation. The solid content of ITO nano-particles in the ink was maintained at 15 wt% in the entire experiment. Ethanol was selected as a solvent for ITO ink. ITO nano-particles were dispersed with a proper dispersant

* Corresponding author. Tel.: +82 10 4579 4432.
E-mail addresses: jihoon.kim@kicet.re.kr, semikjh@gmail.com (J. Kim).

0921-5107/$ – see front matter © 2011 Elsevier B.V. All rights reserved.
doi:10.1016/j.mseb.2011.05.053

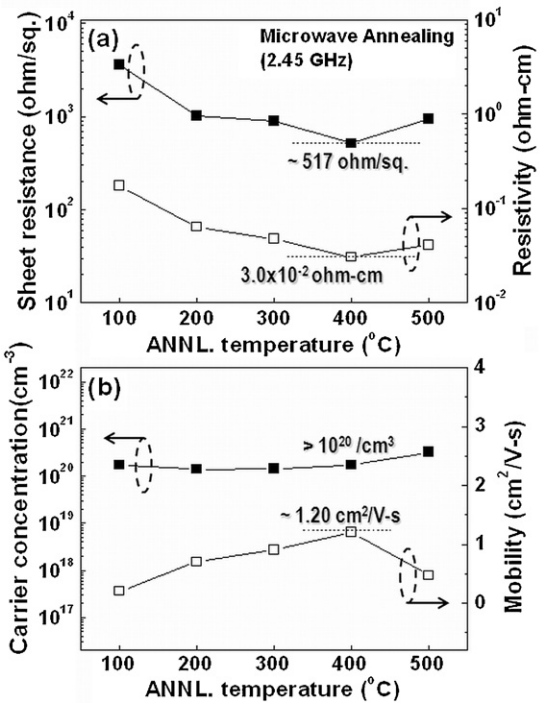

Fig. 1. Electrical properties of inkjet-printed ITO films measured by Hall measurement as a function of microwave annealing temperatures: (a) sheet resistance and resistivity and (b) carrier concentration and mobility.

in the solvent by 72 h ball-mill process. And high speed mixing at 2000 rpm was carried out for 8 min followed by ultrasonic homogenizing process for 10 min. The formulated ITO ink was filtered through a 6 μm polypropylene mesh in order to get rid of agglomerated ITO particles in the ink. The glass substrates were cleaned by acetone, ethanol and boiled isopropanol. UJ 200 inkjet-printing unit (Unijet) was used in the entire experiment, which is equipped with a piezoelectric nozzle with 19 μm orifice from SEMJET (Samsung). The printing frequency, substrate temperature and pitch between ink drops were modulated in order to print uniform ITO films on the substrates. The volume of ink droplet was fixed at 30 pl throughout the entire experiment. The ITO film with the dimension of 20 mm × 20 mm was printed on the glass substrate (25 mm × 25 mm). The inkjet-printed TCO films were annealed in air atmosphere under microwave irradiation (2.45 GHz) with the maximum output power of 2 kW (Unicera; UMF-01). The thickness of the inkjet-printed ITO films was measured by Veeco Dektak 150 surface profiler and field emission scanning electron microscope (FE-SEM; Nova 200). A commercial Ag ink (Advanced Nano Products) was used to print Ag-grid pattern by inkjet. Based on our experiment, the resistivity of the inkjet-printed Ag was less than 10 μΩ-cm with the annealing temperature of 200 °C. The electrical properties of the inkjet-printed ITO films such as sheet resistance and resistivity were measured by Hall measurement (ECOPIA HMS3000). Optical transmittance measurements were implemented using a UV/visible spectrometer (JASCO V-570) in the wavelength ranging from 300 nm to 800 nm.

3. Results and discussion

3.1. Inkjet-printed ITO films

The effects of annealing temperature on sheet resistance, resistivity, carrier mobility, and carrier concentration are presented in Fig. 1. The resistivities of the inkjet-printed ITO films were converted from the sheet resistances with their film thickness values

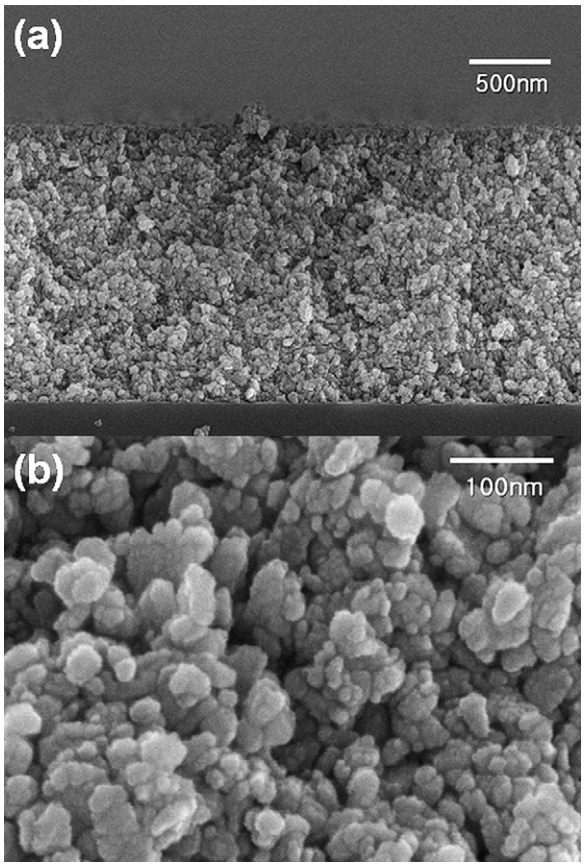

Fig. 2. FE-SEM cross-sectional image of inkjet-printed ITO film: (a) Image magnification = 30,000× and (b) image magnification = 200,000×.

(~580 nm) measured by the surface profiler. The sheet resistances and resistivities of the inkjet-printed ITO films decreased with increasing the annealing temperature since the substitution of In^{3+} with Sn^{4+} as well as the creation of oxygen vacancies in the films were enhanced at the elevated annealing temperatures. The carrier concentrations of the inkjet-printed ITO films were around 10^{20} cm^{-3}, which is comparable to the conventional sputtered ITO films [16]. However, their carrier mobility was 1.2 cm^2/V-s at the best, which is far lower than the sputtered ITO films [16]. In order to investigate the reason for the relatively low carrier mobility in the inkjet-printed ITO films, the microstructure of the films were examined by FE-SEM. Fig. 2 shows the cross-sectional image of the inkjet-printed ITO film after microwave annealing at 400 °C. As presented in Fig. 2, the film comprises nano-particles without a complete connection among them even after the annealing at 400 °C. It indicates that inter-particle scattering of electrons prevails at the interfaces among the nano-particles during their transport along the electric field. The minimum values of the sheet resistance and resistivity from the inkjet-printed ITO films were 517 Ω/sq and 3.0×10^{-2} Ω-cm, respectively after microwave annealing at 400 °C. The sheet resistance and resistivity of the ITO film annealed at 500 °C began to increase due to the decrease in the mobility. Liu et al. indicated that such a reduction in the mobility, even though the carrier concentration still increased after the annealing at 500 °C, is ascribed to the increase in the lattice defects induced from the thermal degradation in the film [18]. It means that, in addition to the inter-particle scattering (Fig. 2), the intra-particle scattering of electrons becomes significant in the film annealed at 500 °C. Further work is in progress aimed at the determination of the mobility degradation mechanism for our inkjet-printed ITO films annealed at the elevated temperatures.

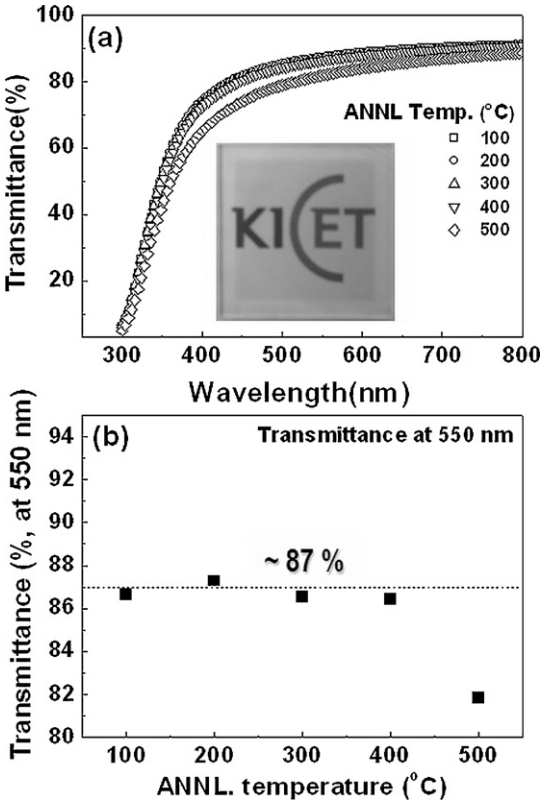

Fig. 3. (a) Optical transmittance spectra of inkjet-printed ITO films within a visible wavelength range are shown as a function of microwave annealing temperatures. The inset presents the image of the inkjet-printed ITO film on the glass. (b) Optical transmittance values at 550 nm are separately plotted.

Fig. 3 compares the optical transmittances of the inkjet-printed ITO films on glass substrates with various annealing temperatures. The inkjet-printed ITO films annealed at different temperatures did not show any significant deviation in the optical transmittance. The optical transmittance values at 550 nm were around 87% regardless of the annealing temperatures less than 400 °C (Fig. 3(b)). The inset in Fig. 3(a) shows the image of a typical inkjet-printed ITO films on a glass substrate. The absorption coefficients (α) of the inkjet-printed ITO films were calculated from the optical transmittance (T) and reflectance (R) data. The optical bandgap for the direct transition of electrons from the valence band to conduction band was related to the absorption coefficient (α) of the inkjet-printed ITO film by the following equations [19]:

$$T = (1 - R)\exp(-\alpha d) \quad (1)$$

$$(\alpha h\nu)^2 = A(h\nu - E_g) \quad (2)$$

where d is the film thickness, E_g is the bandgap of the inkjet-printed ITO films, $h\nu$ is the photon energy, and A is a constant. The change in α^2 as a function of the incident photon energy for the annealing temperatures of the inkjet-printed ITO films is plotted in Fig. 4. The optical bandgap of the inkjet-printed ITO films was obtained by extrapolating the straight segment of each plot onto the photon energy axis at $\alpha = 0$. Fig. 4 indicates that the bandgap values of the inkjet-printed ITO films range from 3.76 eV to 3.82 eV. This range is well matched with the values reported elsewhere [16,19].

3.2. Inkjet-printed ITO/Ag-grid/ITO films

From the previous sections, the lowest values of the sheet resistance and resistivity that the inkjet-printed ITO films reached were 517 Ω/sq and 3.0×10^{-2} Ω-cm after the microwave annealing at

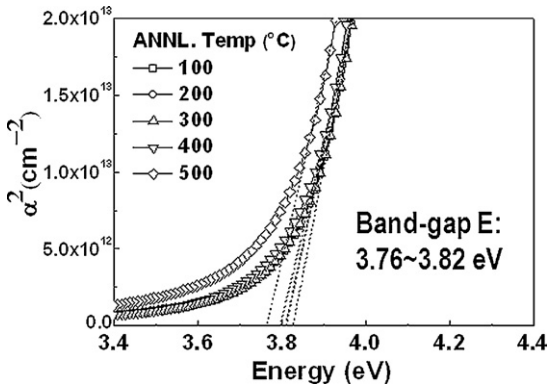

Fig. 4. Optical bandgap energies of inkjet-printed ITO films measured from the transmittance data depending upon microwave annealing temperatures.

400 °C. These values are still one or two orders of magnitude higher than what optoelectronic applications require for TCO films [20]. In order to further reduce down the sheet resistance and resistivity of the inkjet-printed ITO films, Ag-grid pattern was printed by inkjet in between two inkjet-printed ITO films. The width of the printed Ag-grid line was maintained at 50 μm for the entire experiment. The line-to-line pitch of Ag-grid was modulated from 3 mm to 0.5 mm. All three layers (ITO/Ag-grid/ITO) were printed in sequence without breaking the printing process for annealing the individual layer. The annealing process was implemented simultaneously on the entire three layers at 200 °C under microwave. The annealing temperature was decided based on the experimental data that inkjet-printed Ag film is fully sintered at 200 °C, leading to its resistivity less than 10 μΩ-cm. Fig. 5(a) shows the sheet resistance and resistivity of the Ag-grid inserted ITO films as a function of Ag line-to-line pitch.

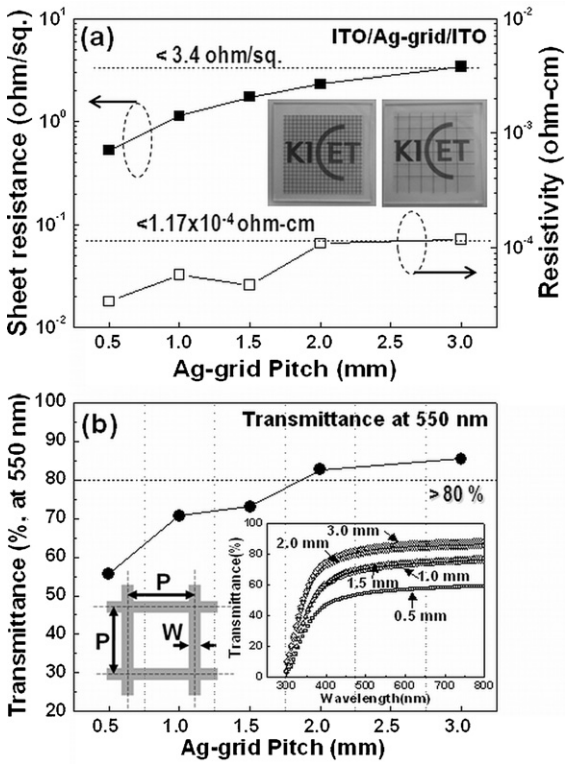

Fig. 5. (a) Electrical properties (sheet resistance and resistivity) of Ag-grid embedded ITO films. The inset image shows the Ag-grid inserted ITO film with 1.0 mm and 3.0 mm Ag-grid pitches. (b) Optical property of Ag-grid embedded ITO films. The inset presents a drawing of the Ag-grid patterns.

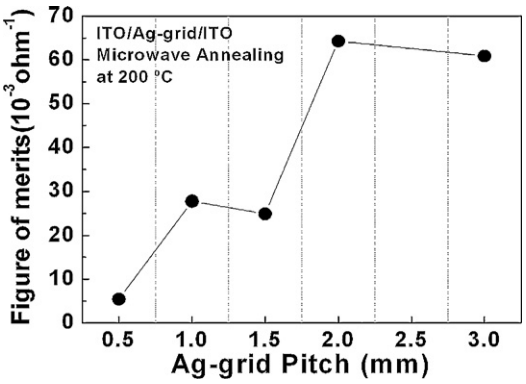

Fig. 6. Figure of merit values for the Ag-grid embedded ITO films as a function of Ag-grid pitch.

The sheet resistance and resistivity of the Ag-grid inserted ITO films significantly decreased with decreasing Ag-grid line pitch. With Ag-grid pitch of 3 mm, both sheet resistance and resistivity value were reduced to 3.4 Ω/sq and 1.17×10^{-4} Ω-cm. These values are two orders of magnitude smaller than the values obtained from the ITO films without Ag-grid. The sheet resistance and resistivity further were decreased down to 0.52 Ω/sq and 3.38×10^{-5} Ω-cm with decreasing the Ag-grid pitch to 0.5 mm. The inset images in Fig. 5(a) present the Ag-grid inserted ITO films with Ag-grid pitches of 1.0 mm and 3.0 mm. Fig. 5(b) shows that the optical transmittance at a wavelength of 550 nm for the Ag-grid inserted ITO films. Their values range from 84% to 55% as Ag-grid pitch decreases from 3.0 mm to 0.5 mm. The insertion of Ag-grid lines in between inkjet-printed ITO films reduced their transmittance values due to the reflection of the incident light at the surface of Ag-grid lines. This reflection is determined by Ag filling factor (F_{Ag}) which quantitatively defines the area covered by Ag-grid lines with respect to non-Ag covered area. F_{Ag} is calculated by $\approx (2 \times W \times P)/P^2$ from the inset of Fig. 5(b) where P is the Ag-grid line-to-line pitch and W is Ag line width. Given that the width of Ag-grid lines is 50 μm, F_{Ag} becomes less than 5% as long as Ag-grid pitch remains wider than 2 mm. It means that less than 5% degradation from the original transmittance value is expected due to the existence of Ag-grid with the pitch wider than 2 mm. Since the transmittance of an inkjet-printed ITO film without Ag-grid was around 87% (Fig. 3), it was expected to have a transmittance higher than 80% from the Ag-grid inserted ITO film. This expectation was well matched with the experimental results presented in Fig. 5(b).

It is evident from Fig. 5 that the sheet resistance and resistivity of Ag-grid inserted ITO films can be improved at the expense of their transparency. In order to optimize the trade-off between transparency and sheet resistance, the figure of merit (ϕ_{FM}), defined by Haacke [21] was introduced:

$$\phi_{FM} = \frac{T^{10}}{R_{sheet}} = \sigma t \ \exp(-10\alpha t) \quad (3)$$

where T is the transmittance at a wavelength of 550 nm, R_{sheet} is the sheet resistance (Ω/sq), σ is the electrical conductivity (Ω^{-1} cm^{-1}), t is the film thickness (cm), and α is the optical absorption coefficient (cm^{-1}). Fig. 6 presents the figure of merit values of Ag-grid inserted ITO films as a function of Ag-grid pitch. It indicates that ϕ_{FM} increases with widening Ag-grid pitch since the increase in the transparency is substantial compared to the increase in the sheet resistance. The maximum ϕ_{FM} value of 64.3×10^{-3} Ω^{-1} was obtained for the Ag-grid inserted ITO film with Ag-grid pitch of 2 mm after microwave annealing at 200 °C. However, the further increase in Ag-grid pitch to 3 mm resulted in the decrease in ϕ_{FM}, indicating that the optimum pitch of Ag-grid was 2 mm for the Ag-grid inserted ITO films. The maximum ϕ_{FM} of the Ag-grid inserted ITO film is comparable to the conventional sputtered ITO films [22], suggesting that the inkjet-printed ITO films with Ag-grid can be applied to various optoelectronic applications.

4. Conclusions

In this paper, inkjet printing of ITO films was investigated. ITO inks were prepared with ITO nano-particles which were mechanically and chemically dispersed in a solvent. The microwave annealing was applied to the films in order to improve their electrical property. The sheet resistance and resistivity of the inkjet-printed ITO films decreased with increasing the annealing temperature. With the annealing at 400 °C, the sheet resistance of 517 Ω/sq was achieved from the film with the thickness of 580 nm. However, the annealing did not affect the optical transmittance of the inkjet-printed ITO films. Ag-grid pattern was printed in between two ITO films in order to further reduce the sheet resistance. With 2 mm Ag line pitch, the Ag-grid inserted ITO film had the sheet resistance less than 3.4 Ω/sq after microwave annealing at 200 °C. The optical transmittance of the Ag-grid ITO film (2 mm Ag-grid pitch) was reduced to 82% compared to the ITO film without Ag-grid (87%) due to the light reflection of Ag-grid. These data suggest that the inkjet-printing approach is a promising process to fabricate transparent conducting oxide films for the future optoelectronic devices and replace the conventional vacuum-based processes.

Acknowledgement

This research was supported by Small & Medium Business Administration (SMBA), Korea under Grant No. S1072318.

References

[1] M. Singh, H.M. Haverinen, P. Dhagat, G.E. Jabbour, Adv. Mater. 22 (2010) 673–685.
[2] H.M. Haverinen, R.A. Myllylä, G.E. Jabbour, Appl. Phys. Lett. 94 (2009) 073108.
[3] H.M. Haverinen, R.A. Myllyä, G.E. Jabbour, J. Disp. Technol. 6 (2010) 87–89.
[4] B.D. Gans, S. Hoeppener, U.S. Schubert, Adv. Mater. 18 (2006) 910–914.
[5] D. Mager, A. Peter, L.D. Tin, E. Fischer, P.J. Smith, J. Hennig, J.G. Korvink, IEEE Trans. Med. Imaging 29 (2010) 482–487.
[6] H. Sirringhaus, T. Kawase, R.H. Friend, T. Shimoda, M. Inbasekaran, W. Wu, E.P. Woo, Science 290 (2000) 2123–2126.
[7] R.A. Stree, W.S. Wong, S.E. Ready, M.L. Chabinyc, A.C. Arias, S. Limb, A. Salleo, R. Lujan, Mater. Today 9 (2006) 32–37.
[8] T. Kawase, H. Sirringhaus, R.H. Friend, T. Shimoda, Adv. Mater. 13 (2001) 1601–1605.
[9] J. Bharathan, Y. Yang, Appl. Phys. Lett. 72 (1998) 2660–2662.
[10] T.R. Hebner, C.C. Wu, D. Marcy, M.H. Lu, J.C. Sturm, Appl. Phys. Lett. 72 (1998) 519–521.
[11] M.A. Aouaj, R. Diaz, A. Belayachi, F. Rueda, M. Abd-Lefdil, Mater. Res. Bull. 44 (2009) 1458–1461.
[12] A. Dippel, T. Schneller, P. Gerber, R. Waser, Thin Solid films 515 (2007) 3797–3801.
[13] T.M. Hammad, Phys. Status Solidi A 206 (2009) 2128–2132.
[14] A. Beaurain, D. Luxembourg, C. Dufour, V. Koncar, B. Capoen, M. Bouazaoui, Thin Solid Films 516 (2008) 4102–4106.
[15] H.W. Jang, J. Kim, H. Kim, Y. Yoon, S. Lee, H. Hwang, J. Kim, Jpn. J. Appl. Phys. 49 (2010) 071501.
[16] H. Kim, C.M. Gilmore, A. Pique, J.S. Horwitz, H. Mattoussi, H. Murata, Z.H. Kafafi, D.B. Chrisey, J. Appl. Phys. 86 (1999) 6451–6461.
[17] X. Zhang, W. Wu, T. Tian, Y. Man, J. Wang, Mater. Res. Bull. 43 (2008) 1016–1022.
[18] D. Liu, C. Sheu, C. Lee, C. Lin, Thin Solid Films 516 (2008) 3196–3203.
[19] H. Han, J.W. Mayer, T.L. Alford, J. Appl. Phys 100 (2006) 083715.
[20] A. Kumar, C. Zhou, ACS Nano 4 (2010) 11–14.
[21] G. Haacke, J. Appl. Phys. 47 (1976) 4086–4089.
[22] J. Jeong, H. Kim, Sol. Energy Mater. Sol. Cells 93 (2009) 1801–1809.